Ultralow-energy All-optical Switches Based on Photonic Crystal Nanocavities

Kengo Nozaki†, Akihiko Shinya, Shinji Matsuo, and Masaya Notomi

Abstract

Photonic crystal cavities having a wavelength-sized volume exhibit a strong light-matter interaction, which makes possible all-optical switches operating with ultralow energy consumption. Using the combination of an extremely small photonic crystal nanocavity and strong carrier-induced nonlinearity in InGaAsP, we have successfully demonstrated low-energy switching in the attojoule range for the first time. This switching energy is more than two orders of magnitude lower than that of previously reported optical switches. The ultrasmall cavity also contributes to fast carrier diffusion and hence a fast switching response of 20 ps at minimum. These all-optical switches with their small size and low-energy, fast-response operation may open up the possibility of a dense photonic network on a chip.

1. Introduction

Photonics has played a key role in the progress of long-haul network links. On the other hand, although data processing at nodes or routers is still performed with integrated electronic circuits, their increasing power consumption and heat generation during high-bitrate operation is now becoming an obstacle to further improvements in network speed and traffic capacity. All-optical data processing with integrated photonic circuits is therefore expected to reduce the amount of power consumed by their electronic counterparts while keeping the high-speed properties of optical signals [1]. However, current photonic processing devices generally require a very high driving energy and are too big for integration, though future interconnect technology will demand micrometer-scale optical components in a chip consuming less than a femtojoule per bit [2]. These problems arise from the difficulty of confining light in a small volume and the weakness of light-matter interactions.

† NTT Basic Research Laboratories
Atsugi-shi, 243-0198 Japan

Photonic crystal (PhC) cavities, which exhibit a high cavity quality factor (Q) and an ultrasmall modal volume (V), are promising candidates as platforms on which to construct devices with dimensions on the order of a few wavelengths of light in matter. Since optical nonlinearities can be greatly enhanced in high-Q, small-V cavities (the optical-field intensity is enhanced in proportion to Q/V), very low operating energy/power can be expected if we apply them to various functional devices. The all-optical switch, which enables gating of an optical signal, should be one of the fundamental elements for constructing photonic circuits [3]–[6], and it is a straightforward example of light-matter interaction enhancement by nanocavities [7]–[9].

A PhC nanocavity is schematically illustrated in **Fig. 1(a)**. A two-dimensional array of airholes is patterned into a semiconductor thin plate having a thickness of ~200 nm. A line defect and a point defect in the array can act as an input/output waveguide and a nanocavity, respectively. The PhC nanocavity can strongly confine light, thereby achieving a strong light-matter interaction and optical nonlinear functionalities [10], [11]. The operating principle of

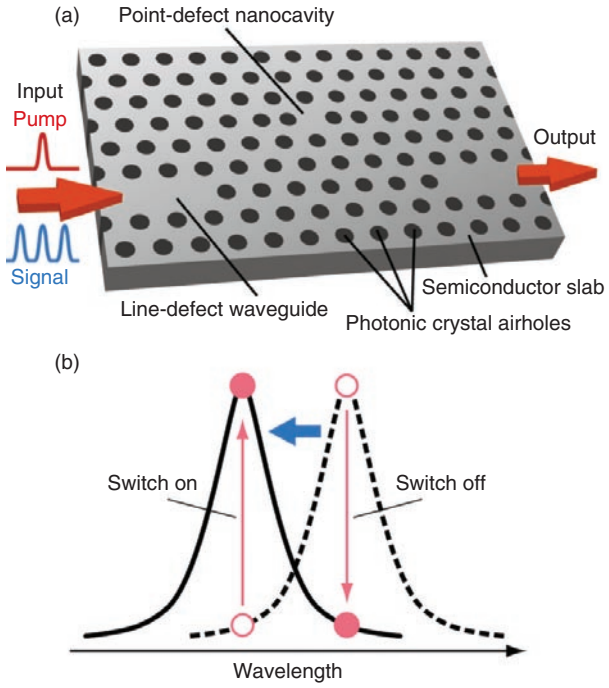

Fig. 1. All-optical switch based on photonic crystal nanocavity. (a) Structural schematic of PhC-nanocavity switch formed in semiconductor (InGaAsP) slab. (b) Operating principle of all-optical switching. Switch-on or switch-off operation is selected by the initial setting of the signal wavelength.

all-optical switching is shown in **Fig. 1(b)**. The pump and signal light pulses are injected into the waveguide simultaneously. The pump light generates carriers in the nanocavity and induces a wavelength shift in the resonant transmission spectrum, which makes it possible to control the signal light output.

This article clarifies the design principle for a PhC-nanocavity-based switch, namely, what type of cavity, nonlinearity, and material we should use. Devices based on our designs exhibit all-optical switching with operating energy in the attojoule range and a time window of a few tens of picoseconds. Our results clearly show that PhC nanocavities enable unprecedented all-optical switches that may lead to high-speed, low-power information processing on a chip.

2. Design

2.1 Smallest PhC cavity

Although we said that a high Q/V ratio is preferable for a lower switching energy, that is a bit too simple. In practice, we need to choose an appropriate Q according to the target operating speed because the photon lifetime in a cavity is proportional to Q. In contrast, cavity volume V should always be as small as possible. In this study, we used a lattice-shifted cavity (hereinafter referred to as an H0 cavity) [12]. The cavity mode consists of only two primary antinodes (**Fig. 2(a)**). Importantly, the H0 cavity has the smallest V among dielectric-core PhC cavities. In our simulation, V was calculated to be only 0.025 μm^3.

Another limiting factor for operating speed is the carrier relaxation time (τ_c). Generally, τ_c is as long as the nanosecond order, but PhC nanocavities offer an efficient way to reduce it. When the cavity becomes ultrasmall, the photogenerated carriers rapidly diffuse out from the cavity, and τ_c becomes small [13]. We numerically solved the carrier diffusion dynamics in a PhC nanocavity. First, we investigated the carrier dynamics without a cavity but assuming an initial Gaussian carrier distribution centered at a certain point in a defect-free PhC lattice. In Fig. 2(a), four black lines show the decay for different initial distribution sizes. They clearly show that a small excitation leads to surprisingly fast diffusion. We investigated more realistic cases with an H0 cavity, as shown by the red line. The fitted τ_c values are as short as 3.5 ps. The time evolution of the carrier distribution for the H0 cavity is shown in **Fig. 2(b)**. The carriers are initially localized in the cavity mode and then start to spread out. This result implies that we can expect a switching bandwidth of nearly 100 GHz. Consequently, it shows that an H0 cavity switch is promising in terms of high-speed response.

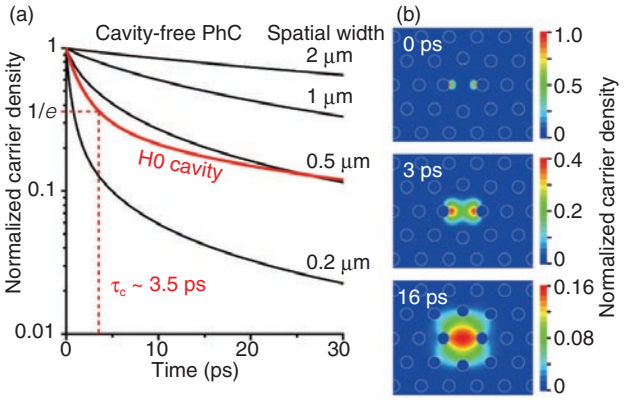

Fig. 2. Simulation results for carrier decay (a) Simulated carrier decay for an H0 cavity (red) and cavity-free PhCs (black). The Gaussian carrier distribution with different spatial widths is set for the cavity-free PhCs. (b) Time evolution of the carrier density distribution for H0 cavity.

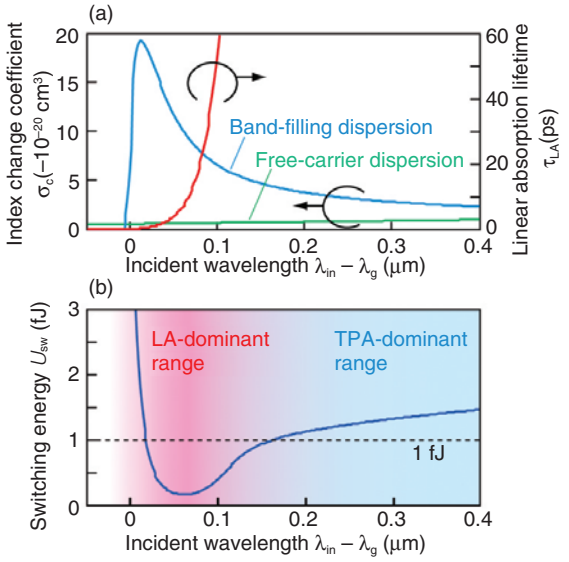

TPA: two-photon absorption

Fig. 3. Material optimization for minimizing switching energy. (a), Index change with carrier density (left axis) and linear absorption lifetime (right axis) as a function of incident wavelength detuning from a bandgap wavelength. (b) Calculated switching energy for parameters of InGaAsP-based H0 cavity.

2.2 Material optimization

To obtain lower switching energy, we want the pump light to be efficiently absorbed in the cavity and the subsequent refractive-index change to be large. InGaAsP is one compound semiconductor that exhibits these features effectively compared with other materials such as Si and GaAs at a wavelength of 1.55 μm.

Figure 3(a) shows the calculated index change and the linear absorption lifetime as a function of the incident wavelength detuning from the bandgap wavelength $\lambda_{in} - \lambda_g$. In our switch, all-optical switching relies on band-filling dispersion (BFD) and free-carrier dispersion in InGaAsP to obtain a refractive index change [14]. Since BFD depends strongly on the position of the electronic band-edge wavelength, we need to find an appropriate InGaAsP composition to suit the cavity's resonant wavelength. On the other hand, optical absorption relies on linear absorption (LA) and nonlinear two-photon absorption (TPA). LA also becomes stronger in the vicinity of the band-edge wavelength and allows efficient absorption. The important point is that excess absorption induces a degradation of cavity Q and increase in switching power, so appropriate adjustment of the composition is needed in order to minimize the switching energy.

The calculated switching energy U_{sw} for the H0 nanocavity is shown in **Fig. 3(b)**. In the vicinity of the band edge, LA boosts the absorption efficiency and BFD enhances the nonlinear resonance shift, thereby effectively reducing U_{sw}. This results in a minimum value of less than 1 fJ at around $\lambda_{in} - \lambda_g = 0.05$ to 0.1 μm. We adjusted the InGaAsP composition to set the photoluminescence peak to 1.47 μm for an operating wavelength of around 1.55 μm.

3. Switching demonstration

3.1 Fabricated H0 nanocavity

We fabricated H0-PhC cavities in an InGaAsP slab using standard top-down processes, including electron-beam lithography and Cl_2-based dry etching. A top-view image of the device is shown in **Fig. 4(a)**. The air-hole diameter, lattice period, and slab thickness are 230, 460, and 200 nm, respectively. The H0 cavity, which was formed by shifting two neighboring air holes by 85 nm in opposite directions, is coupled with input and output PhC waveguides. The transmission spectrum acquired by scanning a wavelength of continuous-wave light is shown in **Fig. 4(b)**. The periodic peaks in the spectrum are not a nanocavity mode, but appear as a result of interference with the Fabry-Pérot resonance caused by the facet end of the waveguide. The fitting curve (black) clarifies the nanocavity mode, indicating that the resonant wavelength λ_{cav} and linewidth are 1567.8 nm and 0.24 nm, respectively. The cavity Q factor is 6500 and the corresponding photon lifetime is $\tau_{ph} = 5.4$ ps, which is slightly longer than the calculated carrier relaxation time of 3.5 ps and is thus unlikely to restrict the switching recovery time.

3.2 Pump-probe measurement

To measure the switching dynamics, we used a degenerate pump-probe technique with an optical pulse width of 14 ps [7], [15]. The center wavelength of the pump pulse was always set to the resonance wavelength, while the wavelength of the probe pulse λ_{probe} was set with detuning $\Delta\lambda_{det} = \lambda_{probe} - \lambda_{cav}$. Switching dynamics for different values of $\Delta\lambda_{det}$ are shown in **Fig. 4(c)**. For $\Delta\lambda_{det} = 0.0$ nm, the transmission of the probe pulse was abruptly switched *off* when the pump pulse temporally overlapped the probe pulse. On the other hand, the probe transmission was switched *on* for $\Delta\lambda_{det} = -0.3$ nm and -0.6 nm

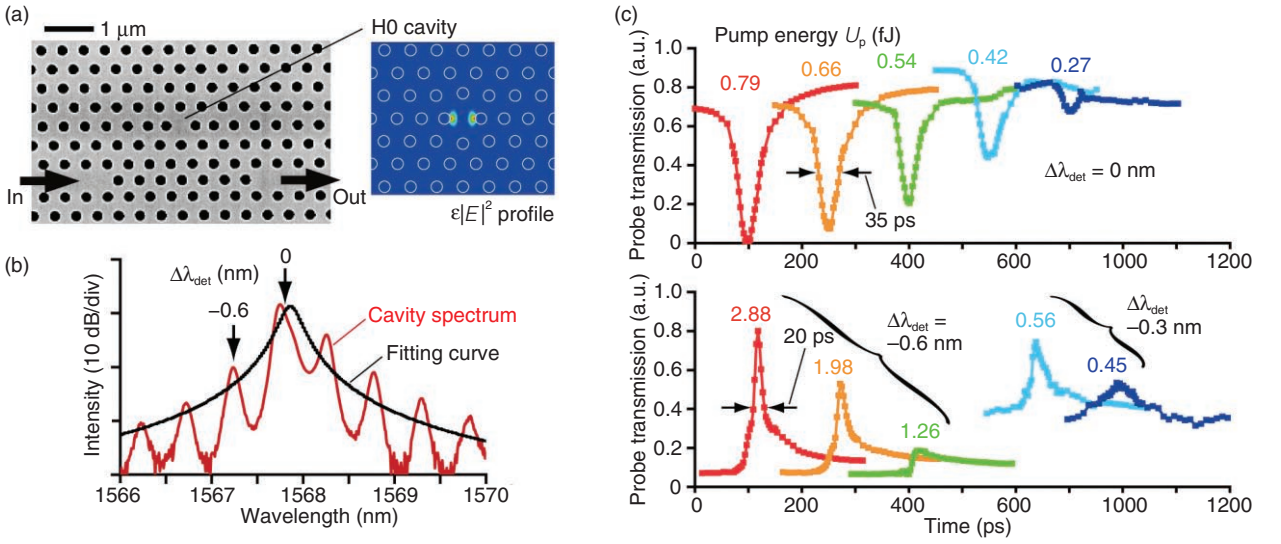

Fig. 4. Switching dynamics of PhC nanocavity acquired by pump-probe measurement. (a) Top-view image and simulated modal distribution of H0 PhC nanocavity. (b) Transmission spectrum scanned with a wavelength-tunable continuous-wave laser. (c) Switching dynamics measured by pump-probe method. Upper and lower plots correspond to results for switch-off and switch-on operations, respectively. Different colors denote results for different pump energies.

because pump-induced carrier nonlinearity induced a resonant blueshift. Switching energies of 420 and 660 aJ were achieved for contrasts of 3 and 10 dB, respectively. These energies are over two magnitudes lower than those reported for Si- and GaAs-based PhC cavities. It should be noted that the switching time window is only 20–35 ps. This value is much shorter than the carrier recombination lifetime (several hundred picoseconds), which is attributable to the rapid carrier diffusion. The improvement in energy and speed is attributed to the ultrasmall size of the cavity and the strong nonlinearity of InGaAsP.

3.3 Gate switching for 40-Gbit/s signal

We performed an experiment in which we extracted a pulse from a repetitive signal train to demonstrate the practicality of our all-optical switches. As shown in **Fig. 5**, we generated a signal train with four pulses with a 25-ps period (40-Gbit/s repetition). We also injected a pump pulse so that it temporally overlapped the second signal pulse to switch it selectively. Output signal pulses show the result of the pulse extraction experiment; they indicate that the second pulse (indicated by an arrow) was selectively switched off or on. These results are promising in terms of the suitability of PhC nanocavity switches for 40-Gbit/s operation.

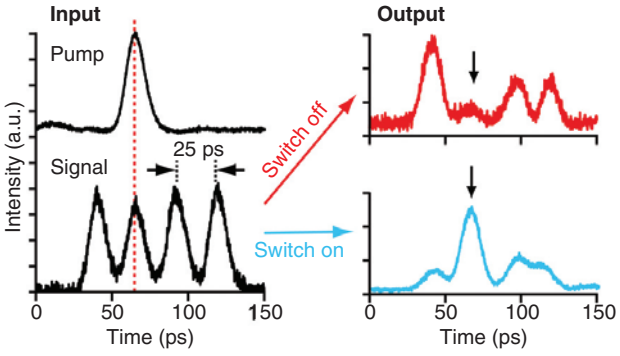

Fig. 5. Gate switching for a signal pulse train at 40 Gbit/s. The pump pulse temporally matches the second signal pulse, and output signals indicate the operations for the switch-off and switch-on regimes.

4. Comparison of all-optical switches

Various all-optical switches are compared in **Fig. 6(a)** in terms of their switching energy per bit and switching time. It is clear that our switch can operate with energy approximately two or more orders of magnitude less than for previously reported ones and has entered the attojoule energy range for the first time. In addition, the previous all-optical switches suffer from a trade-off between switching

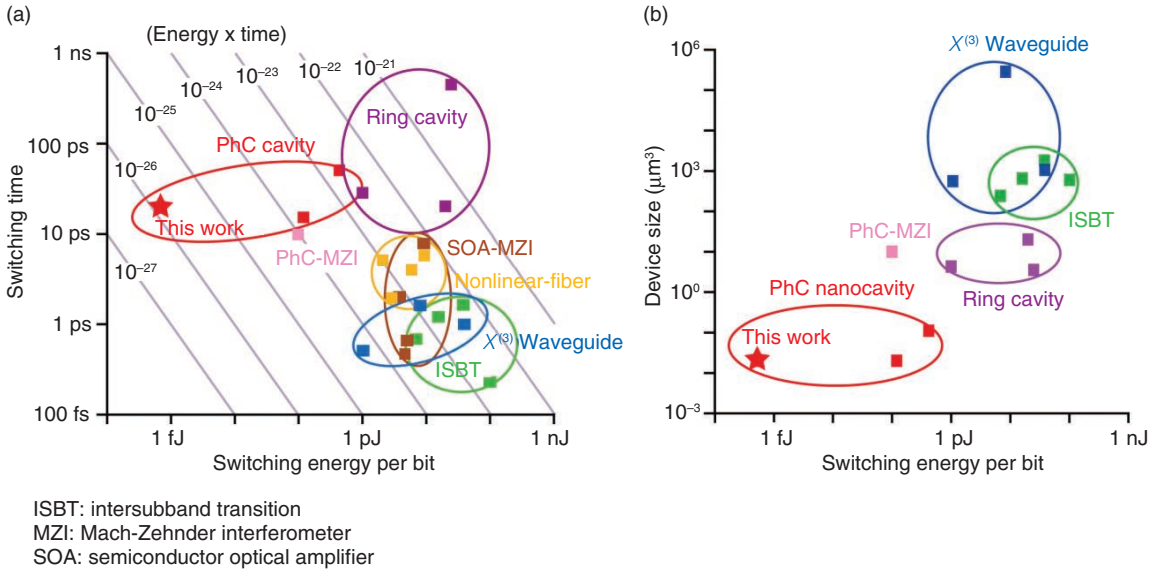

ISBT: intersubband transition
MZI: Mach-Zehnder interferometer
SOA: semiconductor optical amplifier

Fig. 6. Comparison of all-optical switches. (a) Switching time vs. switching energy. (b) Device size vs. switching energy.

time and energy; that is, the energy-time product is limited to around 10^{-24}–10^{-22}. On the other hand, our device clearly overcomes this limitation, exhibiting an energy-time product of 10^{-26}. This is attributed to the ultrasmall size of our cavity. On-chip all-optical switches are compared in **Fig. 6(b)** in terms of switching energy and device size. Our device exhibits both the smallest size and lowest energy. Although all-optical switches involving third-order nonlinearity [16] and inter-subband transition [5], [6] can operate at a much higher bitrate, their high energy consumption and large size might be unacceptable for an on-chip integrated circuit. With our device, assuming 1000 devices on a single chip all operating at a bitrate of 10 Gbit/s, the power consumption is only a few milliwatts. In addition, the ultrasmall size of our device lets us integrate 1000 devices with a small footprint of less than 0.01 mm^2 (assuming a footprint for a single device of less than 10 μm^2). Consequently, the low-power, ultrasmall, and fast PhC-nanocavity switch studied here is unique.

5. Conclusion

We demonstrated all-optical switching with extremely low power consumption using a PhC nanocavity. The achievement of such a densely integrable PhC-nanocavity switch is very important because it will enable low power consumption in the milliwatt range, even in an integrated chip including thousands of devices with a sub-mm^2-order footprint, and it operates at 40 Gbit/s. A wide variety of low-power optical devices, such as optical bistable memory and logic elements [17], [18], should be achievable in a similar way. These PhC-nanocavity-based functionalities are promising for use in optical processing in chip-scale photonic integration.

Acknowledgments

We thank Dr Toshiaki Tamamura of Nano F Consultant (Japan) for help with sample fabrications. This work was partly supported by *Core Research for Evolutional Science and Technology* (CREST) of the Japan Science and Technology Agency (JST).

References

[1] M. Notomi, A. Shinya, K. Nozaki, T. Tanabe, S. Matsuo, E. Kuramochi, T. Sato, H. Taniyama, and H. Sumikura, "Low-power Nanophotonic Devices Based on Photonic Crystals towards Dense Photonic Network on Chip," IET Circuits, Devices & Systems, Vol. 5, No. 2, pp. 84–93, 2011.

[2] D. A. B. Miller, "Device Requirements for Optical Interconnects to Silicon Chips," Proc. of the IEEE, Vol. 97, No. 7, pp. 1166–1185, 2009.

[3] V. R. Almeida, C. A. Barrios, R. R. Panepucci, and M. Lipson, "All-optical Control of Light on a Silicon Chip," Nature, Vol. 431, pp. 1081–1084, 2004.

[4] S. Nakamura, Y. Ueno, and K. Tajima, "Femtosecond Switching with Semiconductor-optical-amplifier-based Symmetric Mach-Zehnder-type All-optical Switch," Appl. Phys. Lett., Vol. 78, No. 25, pp. 3929–3931, 2001.

[5] G. W. Cong, R. Akimoto, K. Akita, T. Hasama, and H. Ishikawa,

"Low-saturation-energy-driven Ultrafast All-optical Switching Operation in (CdS/ZnSe)/BeTe Intersubband Transition," Optics Express, Vol. 15, No. 19, pp. 12123–12130, 2007.
[6] A. V. Gopal, H. Yoshida, A. Neogi, N. Georgiev, T. Mozume, T. Simoyama, O. Wada, and H. Ishikawa, "Intersubband Absorption Saturation in InGaAs-AlAsSb Quantum Wells," IEEE Journal of Quantum Electronics, Vol. 38, No. 11, pp. 1515–1520, 2002.
[7] K. Nozaki, T. Tanabe, A. Shinya, S. Matsuo, T. Sato, H. Taniyama, and M. Notomi, "Sub-femtojoule All-optical Switching Using a Photonic-crystal Nanocavity," Nature Photonics, Vol. 4, pp. 477–483, 2010.
[8] T. Tanabe, M. Notomi, S. Mitsugi, A. Shinya, and E. Kuramochi, "All-optical Switches on a Silicon Chip Realized Using Photonic Crystal Nanocavities," Appl. Phys. Lett., Vol. 87, No. 15, p. 151112, 2005.
[9] C. Husko, A. De Rossi, S. Combrie, Q. V. Tran, F. Raineri, and C. W. Wong, "Ultrafast All-optical Modulation in GaAs Photonic Crystal Cavities," Appl. Phys. Lett., Vol. 94, No. 2, p. 021111, 2009.
[10] M. Notomi, A. Shinya, S. Mitsugi, E. Kuramochi, and H. Y. Ryu, "Waveguides, Resonators and Their Coupled Elements in Photonic Crystal Slabs," Optics Express, Vol. 12, No. 8, pp. 1551–1561, 2004.
[11] M. Notomi, T. Tanabe, A. Shinya, E. Kuramochi, H. Taniyama, S. Mitsugi, and M. Morita, "Nonlinear and Adiabatic Control of High-Q Photonic Crystal Nanocavities," Optics Express, Vol. 15, No. 26, pp. 17458–17481, 2007.
[12] K. Nozaki, S. Kita, and T. Baba, "Room Temperature Continuous Wave Operation and Controlled Spontaneous Emission in Ultrasmall Photonic Crystal Nanolaser," Optics Express, Vol. 15, No. 12, pp. 7506–7514, 2007.
[13] T. Tanabe, H. Taniyama, and M. Notomi, "Carrier Diffusion and Recombination in Photonic Crystal Nanocavity Optical Switches," Journal of Lightwave Technology, Vol. 26, No. 11, pp. 1396–1403, 2008.
[14] B. R. Bennett, R. A. Soref, and J. A. Del Alamo, "Carrier-induced Change in Refractive Index of InP, GaAs, and InGaAsP," IEEE Journal of Quantum Electronics, Vol. 26, No. 1, pp. 113–122, 1990.
[15] D. M. Szymanski, B. D. Jones, M. S. Skolnick, A. M. Fox, D. O'Brien, T. F. Krauss, and J. S. Roberts, "Ultrafast All-optical Switching in AlGaAs Photonic Crystal Waveguide Interferometers," Appl. Phys. Lett., Vol. 95, No. 14, p. 141108, 2009.
[16] C. Koos, P. Vorreau, T. Vallaitis, P. Dumon, W. Bogaerts, R. Baets, B. Esembeson, I. Biaggio, T. Michinobu, F. Diederich, W. Freude, and J. Leuthold, "All-optical High-speed Signal Processing with Silicon-organic Hybrid Slot Waveguides," Nature Photonics, Vol. 3, No. 4, pp. 216–219, 2009.
[17] A. Shinya, S. Matsuo, Yosia, T. Tanabe, E. Kuramochi, T. Sato, T. Kakitsuka, and M. Notomi, "All-optical On-chip Bit Memory Based on Ultra High Q InGaAsP Photonic Crystal," Optics Express, Vol. 16, No. 23, pp. 19382–19387, 2008.
[18] A. Shinya, S. Mitsugi, T. Tanabe, M. Notomi, I. Yokohama, H. Takara, and S. Kawanishi, "All-optical Flip-flop Circuit Composed of Coupled Two-port Resonant Tunneling Filter in Two-dimensional Photonic Crystal Slab," Optics Express, Vol. 14, No. 3, pp. 1230–1235, 2006.

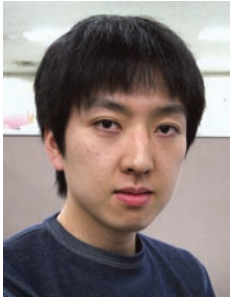

Kengo Nozaki
Research Scientist, Photonic Nanostructure Research Group, Optical Science Laboratory, NTT Basic Research Laboratories.
He received the B.E., M.E., and Ph.D. degrees in electrical and computer engineering from Yokohama National University, Kanagawa, in 2003, 2005, and 2008, respectively. He joined NTT Basic Research Laboratories in 2008. His current interests are all-optical switches, memories, and electro-optic devices based on photonic crystals and related photonic nanostructures. He is a member of the Japan Society of Applied Physics (JSAP).

Shinji Matsuo
Senior Research Engineer, Supervisor, Group Leader of Nano-structure Photonic Devices Research Group, Advanced Opto-electronics Laboratory, NTT Photonics Laboratories.
He received the B.E. and M.E. degrees in electrical engineering from Hiroshima University in 1986 and 1988, respectively, and the Ph.D. degree in electronics and applied physics from Tokyo Institute of Technology in 2008. In 1988, he joined NTT Opto-Electronics Laboratories, where he engaged in research on photonic functional devices using multiple-quantum-well pin modulators and vertical cavity surface-emitting lasers. In 1997, he researched optical networks using wavelength-division multiplexing technologies at NTT Network Innovation Laboratories. Since 2000, he has been engaged in research on high-speed wavelength-tunable lasers for photonic packet switching, frequency-modulated DBR lasers for long-transmission-reach applications, and photonic functional devices using InP/InGaAsP photonic crystal at NTT Photonics Laboratories. He is a member of the IEEE Photonics Society, JSAP, and the Institute of Electronics, Information and Communication Engineers.

Akihiko Shinya
Research Scientist, Photonic Nanostructure Research Group, Optical Science Laboratory, NTT Basic Research Laboratories.
He received the B.E., M.E., and Dr.Eng. degrees in electrical engineering from Tokushima University in 1994, 1996, and 1999, respectively. He joined NTT Basic Research Laboratories in 1999 and has been engaged in R&D of photonic crystal nanodevices. He is a member of JSAP.

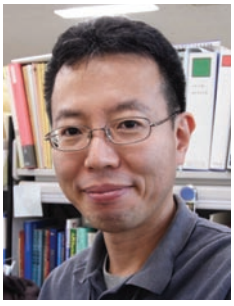

Masaya Notomi
Senior Distinguished Scientist, Group Leader of Photonic Nanostructure Research Group, NTT Basic Research Laboratories.
He received the B.E., M.E., and Ph.D. degrees in applied physics from the University of Tokyo in 1986, 1988, and 1997, respectively. In 1988, he joined NTT Laboratories. Since then, his research interest has been to control the optical properties of materials and devices by using artificial nanostructures and he has been researching quantum wires/dots and photonic crystals. During 1996–1997, he was with Linköping University in Sweden as a visiting researcher. He is also a guest professor of the Department of Physics in Tokyo Institute of Technology. He received the IEEE/LEOS Distinguished Lecturer Award in 2006, JSPS prize in 2009, Japan Academy Medal in 2009, and Commendation for Science and Technology from the Minister of Education, Culture, Sports, Science and Technology in 2010. He is a member of JSAP, the American Physical Society, the Optical Society of America, and IEEE.